



# Observation of zirconium allyl species formed during zirconocene-catalyzed propene polymerization and mechanistic insights



Mihaela Vatamanu\*

Department of Chemistry, Queen's University, Kingston, ON K7L 3N6, Canada

## ARTICLE INFO

### Article history:

Received 15 September 2014

Revised 8 December 2014

Accepted 10 December 2014

### Keywords:

Zirconocene

Allyl species

Mechanism

Stereoerror

Polymerization

3-Propenyl end group

## ABSTRACT

Oligomeric  $\text{Cp}_2\text{Zr}^+$ -allyl species were detected in reaction mixtures of either  $[\text{Cp}_2\text{ZrMe}][\text{MeB}(\text{C}_6\text{F}_5)_3]$  or  $[\text{Cp}_2\text{ZrMe}][\text{B}(\text{C}_6\text{F}_5)_4]$  with propylene by a combination of  $^1\text{H}$  NMR spectroscopy and electrospray ionization (tandem) mass spectrometry techniques. Conjointly, the data imply that formation of  $\text{Cp}_2\text{Zr}^+$ -allyl species occurs via (re)coordination of alkene (propylene and vinylidene end groups of unsaturated polymer chains, respectively) to  $\text{Cp}_2\text{Zr}^+\text{R}$  ( $\text{R} = \text{CH}_3, \text{H}, \text{polymeryl}$ ), followed by intramolecular proton transfer from  $\text{C}\gamma$  to  $\text{R}$  and release of  $\text{RH}$ . Analysis of the olefinic region of the  $^1\text{H}$  NMR spectra of the reaction mixture obtained from  $[\text{Cp}_2\text{ZrMe}][\text{MeB}(\text{C}_6\text{F}_5)_3]$  and propylene reveals the presence of a triplet resonance at  $\delta \sim 5.2$ , which was attributed to the unprecedented 3-propenyl end group. A plausible mechanism for the origin of the 3-propenyl end groups is discussed. Additionally, a mechanism for incorporation of stereodefects into stereoregular polymers is also discussed. The cationic  $\text{Cp}_2\text{Zr}^+$ -allyl intermediates formed during polymerization may contribute to catalyst deactivation.

© 2014 Elsevier Inc. All rights reserved.

## 1. Introduction

Metallocene catalysts of the type  $[\text{Cp}'_2\text{ZrMe}]^+[\text{X}]^-$  ( $\text{Cp}' =$  substituted  $\eta^5$ -cyclopentadienyl group and  $\text{X} =$  weakly coordinating anion) have revolutionized the polyolefin industry, making new polymeric materials possible through precise control of polymer microstructure, composition, and molecular weights [1–5]. The great amount of research conducted in this area to date has resulted in a consensus regarding the main steps of the polymerization reaction [2,6,7]. Thus, it is now established that the active species in these catalysts is the cationic zirconocene alkyl complex  $[\text{Cp}'_2\text{ZrMe}]^+$ , generated in situ via methide abstraction from the catalyst precursor  $\text{Cp}'_2\text{ZrMe}_2$  by a strong Lewis acid. Common Lewis acids include tris(perfluorophenyl)borane and ammonium or trityl salts of  $[\text{B}(\text{C}_6\text{F}_5)_4]^-$  [8–12]. Initiation takes place by coordination of alkene to the vacant site at the metal center, followed by migratory insertion of alkene into the metal–carbon  $\sigma$ -bond. Once the polymerization is initiated, the polymer chain growth occurs by successive alkene coordination and insertion into the  $\text{Zr}-\text{C}$  bond. For  $\alpha$ -alkene (e.g., propylene) polymerizations, insertion of monomer into the  $\text{Zr}-\text{C}$  bond occurs predominantly in a 1,2-fashion to give primary (1,2)  $\text{Zr}$ -polymeryl species, but secondary

(2,1) insertions are also possible. Chain transfer generally involves  $\beta$ -hydride elimination to produce a cationic zirconocene hydride  $[\text{Cp}'_2\text{ZrH}]^+$ , which is able to reinitiate the polymerization and release a polymer chain with an olefinic end group (Scheme 1) [6,7].

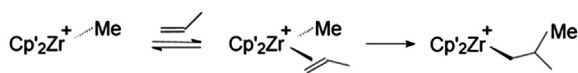
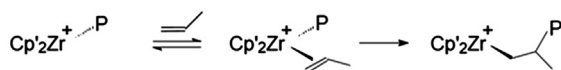
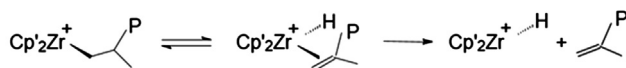
Nevertheless, one aspect of zirconocene-catalyzed alkene polymerization, not yet sufficiently well understood, concerns those incidents that take place during catalysis and impair the catalyst activity and selectivity [3,13–17]. Such occurrences include regio-irregular propylene insertion into the  $\text{Zr}-\text{C}$  bond to form secondary (2,1) zirconium polymeryl species [18–21], formation of zirconium allyl species [22–27], and chain epimerization [28–32].

In a prior publication, it was demonstrated that vinylidene-terminated compounds such as 2,4-dimethyl-1-pentene and 2,4-dimethyl-1-heptene react irreversibly with cationic complexes of the type  $[\text{Cp}_2\text{ZrMe}]^+$  to form mixtures of dynamic isomeric  $\eta^3$  zirconium allyl compounds, which coexist in solution in rapid equilibrium with their  $\eta^1$  counterparts, along with methane [33]. Zirconium allyl complexes have long been presumed to form during  $\alpha$ -olefin polymerization and participate in premature deactivation of the catalyst. Recently, oligomeric zirconium allyl species could actually be observed directly by  $^{13}\text{C}$  NMR spectroscopy in 1- $^{13}\text{C}$ -1-hexene polymerization catalyzed by  $[\text{rac-Me}_2\text{Si}(\text{indenyl})_2\text{ZrCH}_2\text{SiMe}_3][\text{B}(\text{C}_6\text{F}_5)_4]$  [34] and by  $^1\text{H}$  NMR spectroscopy as byproducts in propylene polymerization by  $[\text{Me}_2\text{C}(\text{Cp})(\text{indenyl})\text{Zr}(\text{Me})][\text{MeB}(\text{C}_6\text{F}_5)_3]$  [35]. More recently, by using a

\* Corresponding author. Present address: 100 City Centre Drive, P.O. Box 2225, Mississauga, ON L5B 3C6, Canada.

E-mail address: [vatamanumi@gmail.com](mailto:vatamanumi@gmail.com)



**Initiation:****Propagation:****Chain transfer:**

**Scheme 1.** General mechanism for propylene polymerization by metallocene catalysts ( $\text{Cp}^* = \eta^5\text{-cyclopentadienyl}$  type ligand, P = polypropenyl chain).

combination of NMR and UV–vis spectroscopic techniques, Zr–allyl complexes have also been shown to form during 1-hexene polymerization by  $\text{rac}[\text{Me}_2\text{Si}(1\text{-indenyl})_2\text{ZrMe}_2]$  activated with tritylium perfluorotetraphenylborate in the presence of trimethylaluminum and to constitute about 90% of the total catalyst [36].

In this paper, the results of a series of *in situ* propylene polymerization reactions as catalyzed by  $\text{Cp}_2\text{ZrMe}_2/\text{B}(\text{C}_6\text{F}_5)_3$  [9,10] and  $\text{Cp}_2\text{ZrMe}_2/[\text{Ph}_3\text{C}][\text{B}(\text{C}_6\text{F}_5)_4]$  [37], respectively, are described. The aim of this study is to obtain new experimental evidence that zirconium allyl intermediates form during zirconocene-catalyzed propylene polymerization and to obtain further insights about the chemistry involved in this and in other transformations that might occur during polymerization. A detailed understanding of such transformations is of great importance in the metallocene-catalyzed polymerization of olefins.

## 2. Experimental

### 2.1. General considerations

All chemicals were purchased from Aldrich unless otherwise stated. Deuterated chlorobenzene was purchased from Cambridge Isotope Laboratories (>99% atom% D) and dried by vacuum distillation from  $\text{CaH}_2$ , stored over molecular sieves, and handled in a glove box. Chlorobenzene was dried by distillation under argon from  $\text{CaH}_2$  prior to use. Polymerization-grade propylene (99.5 wt% purity, liquid phase, Praxair) was dried by passage through a column of activated 4 Å molecular sieves prior to use. 2,4-Dimethyl-1-pentene was purchased from ChemSampCo.  $\text{Cp}_2\text{ZrMe}_2$  and  $\text{B}(\text{C}_6\text{F}_5)_3$  were synthesized as described below. Handling and storage of air-/moisture-sensitive organometallic compounds was done using an MBraun LABmaster glove box.

NMR spectra were run on a Bruker AV 600 spectrometer, chemical shifts being referenced using the residual proton signals of the deuterated chlorobenzene. Probe temperatures were calibrated using methanol (low-temperature) and ethylene glycol (high-temperature) samples as references.  $^1\text{H}$  NMR spectra were acquired with a 45° pulse and 1 s delay between pulses; 16 transients were stored for each spectrum. ESI-MS/MS experiments were performed on an MDS Sciex QSTAR XL QqTOF mass spectrometer in ESI positive mode and were run by Dr. Bernd O. Keller.

### 2.2. Synthesis of dimethylzirconocene

Dimethylzirconocene was prepared using a procedure similar to that described in the literature [38,39]. Methylolithium (9 mL, 1.4 M

in diethyl ether) was added dropwise over a period of 45 min to a stirring suspension of zirconocene dichloride (1.75 g, 6 mmol) in 20 mL of dry diethyl ether under argon at  $-20^\circ\text{C}$ , and the reaction mixture thus formed was stirred at this temperature for an additional 30 min. The reaction mixture was then warmed to ambient temperature and the solvent was removed under reduced pressure. The residue was extracted with hexane and filtered, the solvent was evaporated in vacuo, and the product was purified by sublimation at  $70^\circ\text{C}$ . Alternatively, the product was purified by recrystallization from hexane. Dimethylzirconocene was obtained as a white powder at a yield of 60.4%.  $^1\text{H}$  NMR (300 MHz,  $\text{CD}_2\text{Cl}_2$ ):  $\delta$  6.1 (s, 10H, Cp),  $-0.41$  (s, 6H, Me) ppm.  $^1\text{H}$  NMR (400 MHz,  $\text{C}_6\text{D}_5\text{CD}_3$ ):  $\delta$  5.7 (s, 10H, Cp),  $-0.21$  (s, 6H, Me) ppm.

### 2.3. Synthesis of tris(pentafluorophenyl)boron

Tris(pentafluorophenyl)boron was prepared by a modified procedure of Massey and Park [40]. A solution of butyllithium (33 mL, 53 mmol, 1.6 M solution in hexane) was added dropwise over 3 h under argon to a stirred solution of bromopentafluorobenzene (6 mL, 48.1 mmol) in 300 mL dry hexane at  $-78^\circ\text{C}$ . The resulting white suspension was stirred at  $-78^\circ\text{C}$  for an additional 3 h, after which boron trichloride (16 mL, 16 mmol, 1 M solution in hexane) was added all at once and the stirring was continued for another 1 h. After warming to ambient temperature, the reaction mixture was filtered to remove LiCl and the solvent was removed under reduced pressure. Tris(pentafluorophenyl)boron was obtained as white crystals at a yield of 25%.  $^{19}\text{F}$  NMR (400 MHz,  $\text{CD}_2\text{Cl}_2$ ):  $\delta$   $-128$  (br s, 6F, o-F),  $-145$  (t, 3F, p-F),  $-161$  (m, 6F, m-F) ppm.

### 2.4. *In situ* propylene polymerization by $[\text{Cp}_2\text{ZrMe}][\text{MeB}(\text{C}_6\text{F}_5)_3]$

A solution of  $\text{Cp}_2\text{ZrMe}_2$  (40  $\mu\text{mole}$ ) in  $\text{C}_6\text{D}_5\text{Cl}$  (0.5 mL) was added to a solution of  $\text{B}(\text{C}_6\text{F}_5)_3$  (1.1 equiv) in  $\text{C}_6\text{D}_5\text{Cl}$  (0.5 mL) and the yellow ion pair solution thus formed was transferred to an NMR tube. The NMR tube was sealed with a rubber septum and Parafilm and was removed from the glove box, and the ion pair solution was characterized by  $^1\text{H}$  NMR spectroscopy. After the  $^1\text{H}$  NMR, the predetermined amount of propylene was injected into the NMR tube via a syringe at ambient temperature and the NMR tube was shaken vigorously, after which a new  $^1\text{H}$  NMR spectrum was acquired.

### 2.5. *In situ* propylene polymerization by $[\text{Cp}_2\text{ZrMe}][\text{B}(\text{C}_6\text{F}_5)_4]$

A solution of  $\text{Cp}_2\text{ZrMe}_2$  (40  $\mu\text{mole}$ ) in  $\text{C}_6\text{D}_5\text{Cl}$  (0.5 mL) was added to a solution of  $[\text{Ph}_3\text{C}][\text{B}(\text{C}_6\text{F}_5)_4]$  (1.1 equiv) in  $\text{C}_6\text{D}_5\text{Cl}$  (0.5 mL) and the orange ion pair solution thus formed was transferred to an NMR tube. The NMR tube was sealed with a rubber septum and Parafilm and removed from the glove box, and the ion pair solution was characterized by  $^1\text{H}$  NMR spectroscopy. The NMR tube was heated at  $40^\circ\text{C}$  for about 30 min and a new  $^1\text{H}$  NMR spectrum was acquired. The predetermined amount of propylene was injected into the NMR tube via a syringe at ambient temperature and the NMR tube was shaken vigorously, after which another  $^1\text{H}$  NMR spectrum was acquired.

### 2.6. *In situ* reaction between $[\text{Cp}_2\text{ZrMe}][\text{B}(\text{C}_6\text{F}_5)_4]$ and 2,4-dimethyl-1-pentene

A solution of  $\text{Cp}_2\text{ZrMe}_2$  (40  $\mu\text{mole}$ ) in  $\text{C}_6\text{D}_5\text{Cl}$  (0.5 mL) was added to a solution of  $[\text{Ph}_3\text{C}][\text{B}(\text{C}_6\text{F}_5)_4]$  (1.1 equiv) in  $\text{C}_6\text{D}_5\text{Cl}$  (0.5 mL) and the orange ion pair solution thus formed was transferred to an NMR tube. The NMR tube was sealed with a rubber septum and Parafilm and removed from the glove box. Before the NMR spectrum was determined, 2,4-dimethyl-1-pentene (1.0–1.5



equiv) was injected into the NMR tube at ambient temperature via a microsyringe. The reaction products could not be isolated and were characterized in solution by  $^1\text{H}$  NMR and correlation spectroscopy.

### 2.7. NMR spectroscopic data of $[\text{Cp}_2\text{Zr}(\eta^3\text{-CH}_2\text{C}(\text{CH}_2\text{CHMe}_2)\text{CH}_2)]^+[\text{B}(\text{C}_6\text{F}_5)_4]^-$

$^1\text{H}$  NMR (600 MHz,  $\text{C}_6\text{D}_5\text{Cl}$ ,  $0^\circ\text{C}$ ):  $\delta$  5.71 (s,  $\text{C}_5\text{H}_5$ , 5H), 5.60 (s,  $\text{C}_5\text{H}_5$ , 5H), 3.38 (s, allyl  $\text{H}_a$ , 2H), 2.56 (s, allyl  $\text{H}_b$ , 2H), 1.96 (d,  $\text{CH}_2$ ,  $^3J_{\text{HH}} = 6.5$  Hz, 2H), 1.76 (m, CH, 1H), 1.01 (d,  $\text{CH}_3$ ,  $^3J_{\text{HH}} = 6.5$  Hz, 6H) ppm.

$^{13}\text{C}$  NMR (600 MHz,  $\text{C}_6\text{D}_5\text{Cl}$ ,  $0^\circ\text{C}$ ):  $\delta$  112.8 ( $\text{C}_5\text{H}_5$ ,  $^1J_{\text{C-H}} = 171$  Hz),  $\delta$  111.2 ( $\text{C}_5\text{H}_5$ ,  $^1J_{\text{C-H}} = 171$  Hz), 68.5 (allyl  $\text{CH}_2$ ,  $^1J_{\text{C-Ha}} = 145$  Hz,  $^1J_{\text{C-Hb}} = 156$  Hz), 163.6 (allyl C), 53 ( $\text{CH}_2$ ,  $^1J_{\text{C-H}} = 135$  Hz), 31.2 (CH,  $^1J_{\text{C-H}} = 127$  Hz), 23 ( $\text{CH}_3$ ,  $^1J_{\text{C-H}} = 129$  Hz) ppm.

### 2.8. NMR spectroscopic data of $[\text{Cp}_2\text{ZrMe}]^+[\text{MeB}(\text{C}_6\text{F}_5)_3]^-$

$^1\text{H}$  NMR (600 MHz,  $\text{C}_6\text{D}_5\text{Cl}$ ,  $25^\circ\text{C}$ ):  $\delta$  5.97 (s,  $\text{C}_5\text{H}_5$ , 10H), 0.56 (s,  $\text{Zr-CH}_3$ , 3H), 0.34 (br.s,  $\text{B-CH}_3$ , 3H) ppm.

$^1\text{H}$  NMR (600 MHz,  $\text{C}_6\text{D}_5\text{Cl}$ ,  $0^\circ\text{C}$ ):  $\delta$  5.93 (s,  $\text{C}_5\text{H}_5$ , 10H), 0.55 (s,  $\text{Zr-CH}_3$ , 3H), 0.33 (br.s,  $\text{B-CH}_3$ , 3H) ppm.

### 2.9. General procedure for variable-temperature NMR experiments

The procedure used for variable-temperature NMR experiments is similar to that described in the literature [33]. Samples of  $[\text{Cp}_2\text{Zr}^+(\eta^3\text{-C}_3\text{H}_4)\text{CH}_2\text{CHMe}_2][\text{B}(\text{C}_6\text{F}_5)_4]^-$  used for variable-temperature  $^1\text{H}$  NMR studies were prepared as described above. Samples were brought to the indicated temperature and allowed to equilibrate for 7–10 min before the  $^1\text{H}$  NMR spectra were acquired. All of the temperature-dependent changes are reversible; i.e., on cooling the probe temperature, the reverse chemical shift changes occur. Free energy of activation,  $\Delta G^\ddagger$ , was calculated in kJ/mol from the equation  $\Delta G^\ddagger = R \cdot T[23.76 - \ln(k/T)]$ , where  $R$  is the gas constant (8.3145 J/mol K),  $T$  is the absolute temperature (K), and  $k$  is the rate constant ( $\text{s}^{-1}$ ) [41].

### 2.10. General procedure for ESI-MS/MS experiments

A solution of  $\text{Cp}_2\text{ZrMe}_2$  (40  $\mu\text{mol}$ ) in dry chlorobenzene (0.5 mL) was added to a solution of  $\text{B}(\text{C}_6\text{F}_5)_3$  (1.1 equiv) in dry chlorobenzene (0.5 mL) and the yellow ion pair solution thus formed was transferred to a vial. The vial was sealed with a rubber septum and Parafilm and removed from the glove box and a predetermined amount of propylene (5–10 equiv) was injected into the NMR tube

via a syringe at ambient temperature. The vial was quickly shaken, the reaction mixture was further diluted with an additional 1 mL of dry chlorobenzene and shaken again. The resulted reaction mixture was then fed continuously into the first quadrupole of a QSTAR XL QqTOF mass spectrometer, under an atmosphere of dry nitrogen, via a syringe. The flow rate could be varied between 5 and 20  $\mu\text{L}/\text{min}$ .

## 3. Results and discussion

### 3.1. Reaction of propylene with $[\text{Cp}_2\text{ZrMe}]^+[\text{MeB}(\text{C}_6\text{F}_5)_3]^-$

The  $[\text{Cp}_2\text{ZrMe}]^+[\text{MeB}(\text{C}_6\text{F}_5)_3]^-$  ion pair (**1**), generated in situ by reacting  $\text{Cp}_2\text{ZrMe}_2$  with a slight excess (1.1 equiv) of  $\text{B}(\text{C}_6\text{F}_5)_3$  in chlorobenzene- $\text{d}_5$  at ambient temperature, was reacted with 5–10 equiv of propylene. The  $^1\text{H}$  NMR spectra of the reaction mixtures recorded following addition of propylene reveal rapid and quantitative conversion of propylene to short-chain atactic polypropylene oligomers, as indicated by the presence of the backbone  $-\text{CH}_2\text{CH}(\text{Me})_n-$  resonances in the aliphatic ( $\delta$  0.7–2.2) region of the spectra, while free propylene [42] resonances are missing (Fig. 1). Small quantities of unreacted **1** ( $\delta$  5.97 (Cp) and  $\delta$  0.56 (Zr-Me)) are still present when 5 equiv of propylene are used, which indicates that chain propagation is faster than initiation (i.e., the first propylene insertion into the Zr-Me bond). The Me-B ( $\delta$  0.34) resonance is not evident any more, and it seems reasonable that it overlaps with the backbone polypropylene oligomer resonances after being shifted downfield toward a free  $[\text{MeB}(\text{C}_6\text{F}_5)_3]^-$  ( $\delta$  1.1–1.2) resonance [33]. The  $^1\text{H}$  NMR spectra of the reaction mixtures also show the presence of a series of low-relative-intensity resonances in the Cp region between  $\delta$  5.9 and 6.4, in addition to the olefinic group resonances [43,44] present between  $\delta$  4.8 and 5.4. While no attempt to identify these resonances was made, it seems reasonable that they belong to the Cp hydrogens of various  $\text{Cp}_2\text{Zr}^+$ -polypropenyl species present in the reaction mixture (vide infra).

Notable, however, are the low-intensity, exchange-broadened resonances detected in the allylic ( $\delta$  2.5–4.8) and Cp ( $\delta$  ~5.7) regions of the  $^1\text{H}$  NMR spectra and a sharp singlet at  $\delta$  0.25 attributable to methane. Owing to the close similarity to the previously reported  $^1\text{H}$  NMR spectra of related complexes used as model compounds [33], these resonances were attributed to the allylic and Cp hydrogens, respectively, of various oligomeric Zr-allyl intermediates of the type  $[\text{Cp}_2\text{Zr}(\eta^3\text{-CH}_2\text{C}(\text{CH}_2\text{P})\text{CH}_2)]^+$  and  $[\text{Cp}_2\text{Zr}(\eta^3\text{-CH}_2\text{C}(\text{Me})\text{CHP})]^+$  (P = short chain alkyl or polymeryl group) formed during the propylene oligomerization reaction.

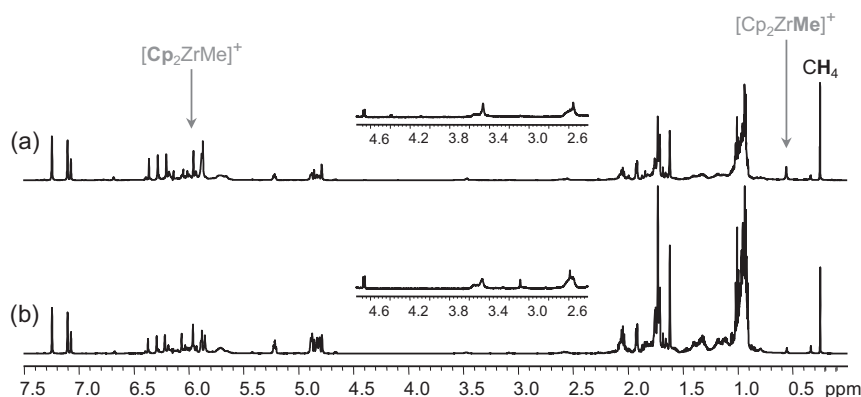


Fig. 1.  $^1\text{H}$  NMR spectra of in situ propylene oligomerization by **1** in chlorobenzene- $\text{d}_5$  (ambient temperature, 600 MHz): (a) after addition of 5 equiv of propylene, (b) after addition of 10 equiv of propylene. Insets show the allylic region.



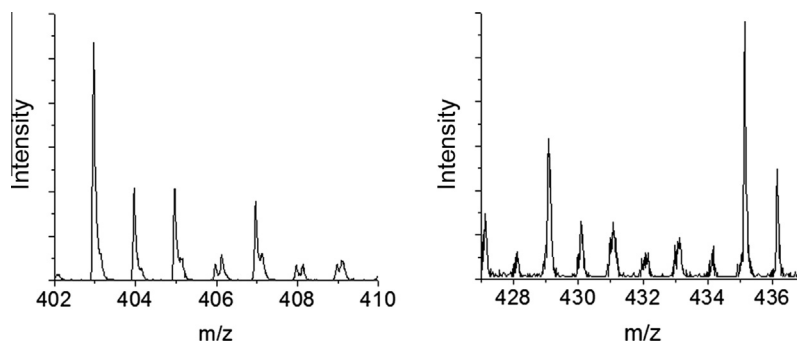


Fig. 2. Positive mode ESI-MS spectra of molecular ions of  $m/z$  403 corresponding to  $[\text{Cp}_2\text{Zr}(\text{C}_3\text{H}_6)_4\text{CH}_3]^+$  and  $m/z$  429 corresponding to  $[\text{Cp}_2\text{Zr}(\text{C}_3\text{H}_4)(\text{C}_3\text{H}_6)_4\text{H}]^+$ .

In any case, the allylic region of the  $^1\text{H}$  NMR spectra in Fig. 1 looks complicated because of the presence of different chain length  $\text{Cp}_2\text{Zr}^+$ -allyl oligomers, in addition to the inter- and intramolecular exchange processes [33] associated with these zirconium allyl complexes in solution, and as a result, clear identification of particular zirconium allyl intermediates by  $^1\text{H}$  NMR spectroscopy is difficult. To identify individual oligomeric  $\text{Cp}_2\text{Zr}^+$ -allyl species present in the catalytic system, the reaction of propylene with **1** was also investigated using electrospray ionization (tandem) mass spectrometry. Unlike  $^1\text{H}$  NMR spectroscopy, this technique allows the identification of individual  $\text{Cp}_2\text{Zr}^+$ -containing intermediates present in a reaction mixture by mass-to-charge ratio ( $m/z$ ).

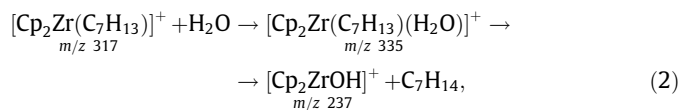
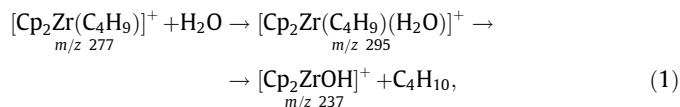
In a typical experiment, 5 equiv of propylene was added to a solution of **1** ( $4 \times 10^{-2}$  M) in chlorobenzene at ambient temperature. The resulted reaction mixture was further diluted twofold with chlorobenzene and then fed continuously into the first quadrupole of a QSTAR XL QqTOF mass spectrometer via an electrospray ionization interface. The electrospray ionization technique is known to release molecular ions preformed in solution with very little or no fragmentation [45,46]. The electrospray ionization mass spectrometry (ESI-MS) spectra of the reaction mixture obtained in the positive ion mode by scanning the first quadrupole were complex and of low quality because of many overlapping peaks of the  $\text{Cp}_2\text{Zr}^+$ -containing species with only small differences in their molecular ion masses.

Indeed, a typical ESI-MS spectrum of a cationic zirconocene complex displays a distinct isotopic pattern of seven peaks, due to the contributions of the five principal natural isotopes of zirconium and along with the natural isotopes of carbon and hydrogen [47]. Shown in Fig. 2 are the positive mode ESI-MS spectra for peaks at  $m/z$  403 and 429 with isotopic patterns corresponding to  $[\text{Cp}_2\text{Zr}(\text{C}_3\text{H}_6)_4\text{CH}_3]^+$  and  $[\text{Cp}_2\text{Zr}(\text{C}_3\text{H}_4)(\text{C}_3\text{H}_6)_4\text{H}]^+$ , respectively. Nevertheless, due to the large variety of  $\text{Cp}_2\text{Zr}^+$ -containing reaction intermediates that can form during the polymerization, which can differ by an  $m/z$  less than 7, extensive overlapping of peaks occurred. In addition, the complexity of the ESI-MS spectra was further enhanced by some decomposition of the reaction intermediates due to the traces of water and other contaminants present in the instrument. Therefore, direct identification of various oligomeric zirconocene intermediates present in the reaction mixture on the basis of their natural isotope distribution pattern is difficult.

In order to identify the cationic  $\text{Cp}_2\text{Zr}^+$  intermediates of interest, specific  $m/z$  peaks corresponding to particular molecular zirconocene complexes were isolated from the first quadrupole and further examined by collision-induced dissociation (CID) experiments. A single  $m/z$  value, corresponding to the cationic  $\text{Cp}_2\text{Zr}^+$ -containing species having the most abundant  $^{90}\text{Zr}$  isotope, was selected for each particular zirconocene complex. Fig. 3 displays the molecular ion distribution for the cationic zirconocene alkyl  $\text{Cp}_2\text{Zr}^+(\text{C}_3\text{H}_6)_n\text{CH}_3$  ( $n = 1-6$ ) and cationic zirconocene allyl  $\text{Cp}_2\text{Zr}^+$

$(\text{C}_3\text{H}_4)(\text{C}_3\text{H}_6)_n\text{CH}_3$  ( $n = 0-5$ ) species, respectively, selected from the first quadrupole, together with detailed electrospray ionization tandem mass (ESI-MS/MS) spectra of two selected molecular ions.

As can be seen from the insets of Fig. 3, the selected molecular ions of  $m/z$  277, corresponding to  $\text{Cp}_2\text{Zr}^+(\text{C}_4\text{H}_9)$ , and  $m/z$  317, corresponding to  $\text{Cp}_2\text{Zr}^+(\text{C}_7\text{H}_{13})$ , show loss of the alkyl and allyl ligands, respectively, to yield a signal of  $m/z$  220 corresponding to the  $[\text{Cp}_2\text{Zr}]^+$  fragment ion. The  $[\text{Cp}_2\text{Zr}]^+$  fragment ion is diagnostic for identification of a zirconocene complex [46,47]. Also present in the  $\text{Cp}_2\text{Zr}^+(\text{C}_4\text{H}_9)$  and  $\text{Cp}_2\text{Zr}^+(\text{C}_7\text{H}_{13})$  tandem mass spectra are the molecular ions of  $m/z$  295 and 335, which could be attributed to the  $[\text{Cp}_2\text{Zr}(\text{C}_4\text{H}_9)(\text{H}_2\text{O})]^+$  and  $[\text{Cp}_2\text{Zr}(\text{C}_7\text{H}_{13})(\text{H}_2\text{O})]^+$  adduct ions, respectively, and a molecular ion of  $m/z$  237 corresponding to the  $[\text{Cp}_2\text{ZrOH}]^+$  complex [48]. These are byproducts formed in the collision cell from the reaction of the corresponding zirconocene cations with traces of water present in the instrument,



and their presence in these spectra, although unfortunate, also attests the presence of the cationic zirconocene species of interest. The ESI-MS/MS spectra of all selected molecular ions are similar in nature. Likewise, cationic  $\text{Cp}_2\text{Zr}^+(\text{C}_3\text{H}_6)_n\text{H}$  ( $n = 1-5$ ,  $m/z$  263, 305, 347, 389, 431) and  $\text{Cp}_2\text{Zr}^+(\text{C}_3\text{H}_4)_n\text{H}$  ( $m/z$  261) were also detected.

Note that traces of water and other contaminants present in the instrument would inevitably react with both cationic  $\text{Cp}_2\text{Zr}^+$ -allyl and  $\text{Cp}_2\text{Zr}^+$ -alkyl complexes, thus lowering their molecular ion peak intensities in the acquired ESI-MS/MS spectra. On the other hand, a small contribution to the intensity of oligomeric  $\text{Cp}_2\text{Zr}^+$ -allyl peaks can come from a  $\text{Cp}_2\text{Zr}^+$ -polypropenyl species bearing an internal unsaturation (vide infra). Hence, this investigation focuses only on qualitative identification of the oligomeric zirconocene allyl and alkyl intermediates present in the reaction mixture and does not provide quantitative information about these species.

Cationic  $\text{Cp}_2\text{Zr}^+$ -polymeryl intermediates have been observed previously in gas-phase reaction of  $\text{Cp}_2\text{Zr}^+$ -Me with ethylene and 1-butene, respectively, by ESI-MS and ESI-MS/MS [46,49]. Also, cationic  $\text{Cp}_2\text{Zr}^+$ (allyl) complexes were formerly detected by tandem mass spectrometry as the main reaction products of corresponding Zr-polymeryl species in the CID experiments via loss of  $\text{H}_2$  [46]. However, the direct identification of oligomeric  $\text{Cp}_2\text{Zr}^+$ -polypropenyl and  $\text{Cp}_2\text{Zr}^+$ -allyl intermediates preformed in solution under



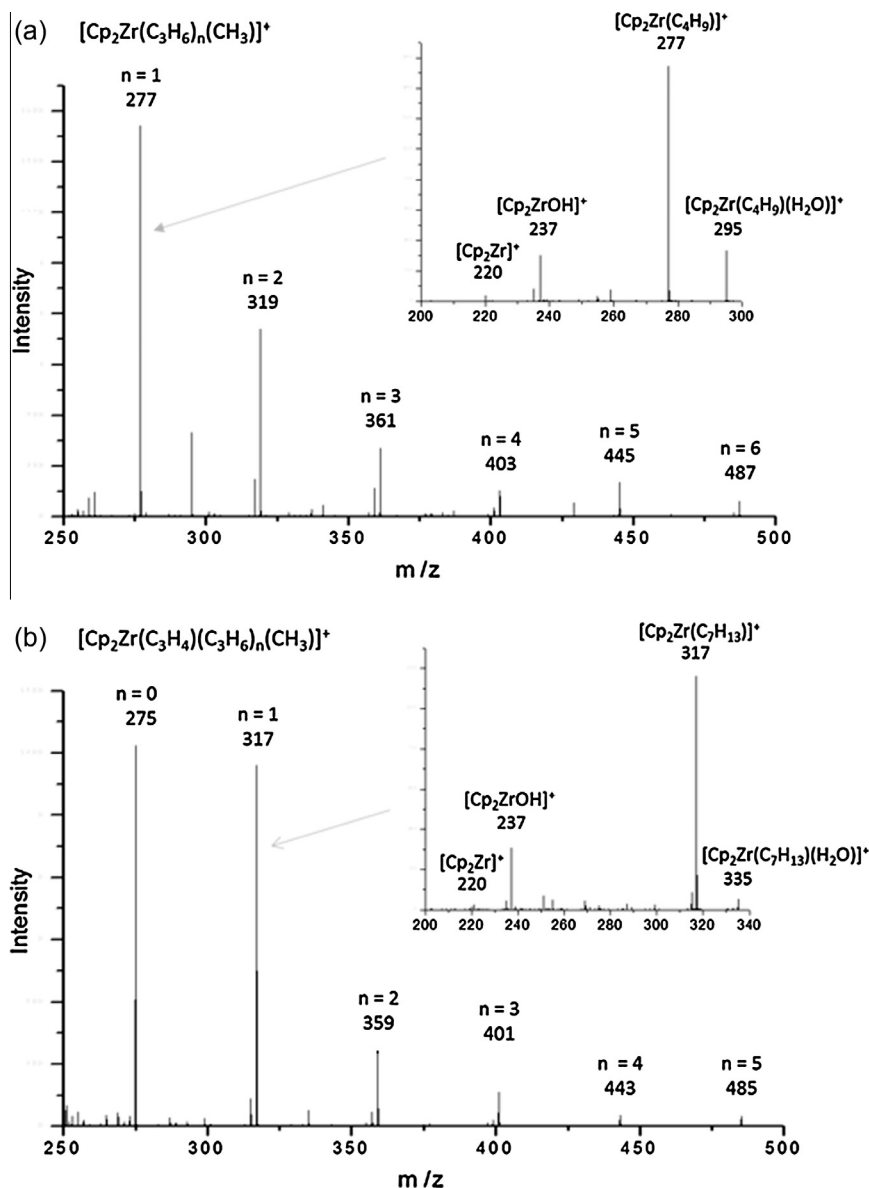


**Fig. 3.** The molecular ion distributions for (a)  $\text{Cp}_2\text{Zr}^+(\text{C}_3\text{H}_6)_n\text{CH}_3$  ( $n = 1-6$ ) and (b)  $\text{Cp}_2\text{Zr}^+(\text{C}_3\text{H}_4)(\text{C}_3\text{H}_6)_n\text{CH}_3$  ( $n = 0-5$ ). Insets in (a) and (b) show fragmentation of ions of  $m/z$  277 and 317, respectively.

catalytic conditions by electrospray ionization (tandem) mass spectrometry has not been reported previously.

### 3.2. Reaction of propylene with $[\text{Cp}_2\text{ZrMe}][\text{B}(\text{C}_6\text{F}_5)_4]$

The analogous reaction engaging  $[\text{Ph}_3\text{C}][\text{B}(\text{C}_6\text{F}_5)_4]$  as a cocatalyst was similarly investigated by  $^1\text{H}$  NMR spectroscopy.  $\text{Cp}_2\text{ZrMe}_2$  was reacted with 1.1–1.2 equiv of  $[\text{Ph}_3\text{C}][\text{B}(\text{C}_6\text{F}_5)_4]$  in chlorobenzene- $d_5$  at ambient temperature to generate the corresponding ion pair  $[\text{Cp}_2\text{ZrMe}][\text{B}(\text{C}_6\text{F}_5)_4]$  (**2**) and  $\text{Ph}_3\text{CMe}$ . Small quantities of methyl-bridged binuclear cations  $[(\text{Cp}_2\text{ZrMe})_2(\mu\text{-Me})]^+$  were also formed [8,50], and they were slowly converted to the mononuclear species **2** and the catalyst precursor  $\text{Cp}_2\text{ZrMe}_2$  by warming the NMR tube at  $40^\circ\text{C}$  for 30 min [50]. Treatment of a chlorobenzene- $d_5$  solution of **2** with 5–10 equiv of propylene at ambient temperature resulted in rapid and complete conversion of propylene to low-molecular-weight polypropylene chains; however, compared with the previous example where the initial cationic zirconocene catalyst  $[\text{Cp}_2\text{ZrMe}]^+$  was basically consumed after

addition of 10 equiv of propylene, here a majority (about 60% as determined by  $^1\text{H}$  NMR spectroscopy using  $\text{Ph}_3\text{CMe}$ , present in the reaction solution, as an internal standard) of the initial catalyst  $[\text{Cp}_2\text{ZrMe}]^+$  remained unconsumed (Fig. 4), consistent with prior observations that the propagation rate is higher when an anion with a weaker coordinating ability is used [51,52].

As can be seen in Fig. 4, aside from the  $[\text{Cp}_2\text{ZrMe}]^+$  ( $\delta$  5.99 (Cp) and 0.78 (Zr–Me)),  $\text{Ph}_3\text{CMe}$  ( $\delta$  2.13 (Me) and  $\delta$  7.1–7.4 (Ph)) and the expected backbone  $-\text{CH}_2\text{CHMe}-$  ( $\delta$  0.9–2.0) resonances, the  $^1\text{H}$  NMR spectra of the reaction mixtures obtained following addition of propylene also show the presence of two low-intensity resonances with an approximately 1:1 ratio of intensities at  $\sim\delta$  5.7 and 5.8, a series of weak resonances in the allyl region between  $\delta$  2.5 and 4.7, and a resonance at  $\delta$  0.25 ascribed to methane. On the basis of comparison with literature precedents [33], in addition to the above-described  $^1\text{H}$  NMR spectra (Fig. 1), the resonances present in the Cp ( $\sim\delta$  5.7, 5.8) and allyl ( $\delta$  2.5–4.7) regions were attributed to the Cp and allyl hydrogens of oligomeric  $\text{Cp}_2\text{Zr}^+$ -allyl species existing in the reaction mixture. However, the observation



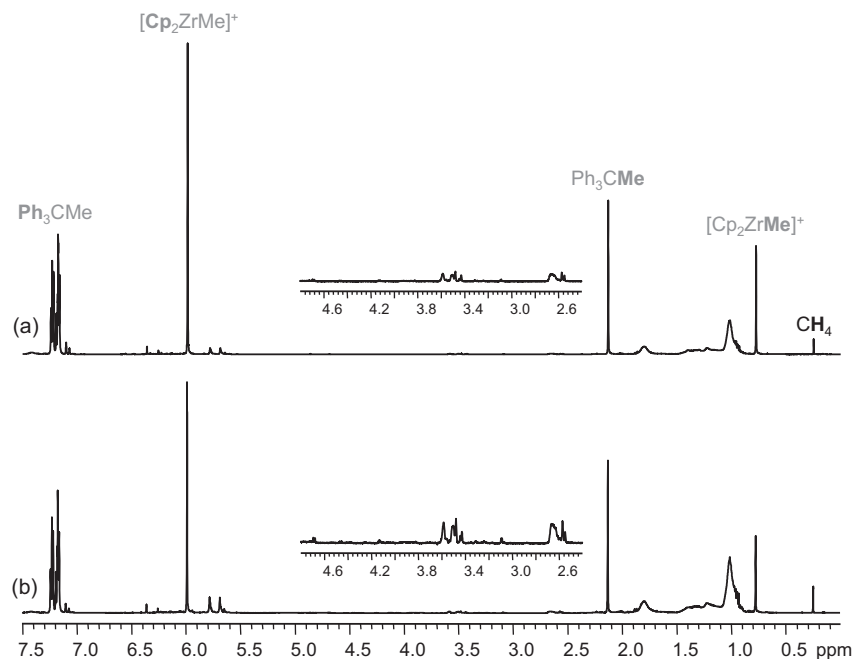


**Fig. 4.**  $^1\text{H}$  NMR spectra of in situ propylene oligomerization by **2** in chlorobenzene- $d_5$  (ambient temperature, 600 MHz): (a) after addition of 5 equiv of propylene, (b) after addition of 10 equiv of propylene. Insets show the allylic region.

of two Cp resonances for the oligomeric  $\text{Cp}_2\text{Zr}^+$ -allyl intermediates in the present case stands in marked contrast with the preceding findings (*vide supra*) in which only one broad Cp resonance was observed, and implies a relatively static structure of the  $\eta^3$ -allyl ligand of the oligomeric  $\text{Cp}_2\text{Zr}^+$ -allyl species with respect to the  $\text{Cp}_2\text{Zr}^+$  unit under these conditions. This difference in dynamics of the allyl ligands of oligomeric  $\text{Cp}_2\text{Zr}^+$ -allyl complexes could be related to the different coordination ability of the anions as well.

To determine whether the anion actually has such an effect on the dynamic behavior of the  $\text{Cp}_2\text{Zr}^+$ -allyl species, the in situ reaction between the catalyst **2** and 2,4-dimethyl-1-pentene (1.0–1.5 equiv), used as a model compound for a vinylidene-terminated polymer chain, was also performed under otherwise identical conditions. As expected, the  $^1\text{H}$  NMR spectrum of the resulted zirconocene allyl complex  $[\text{Cp}_2\text{Zr}^+(\eta^3\text{-C}_3\text{H}_4)\text{CH}_2\text{CHMe}_2][\text{B}(\text{C}_6\text{F}_5)_4]$  (**3**), at ambient temperature, is similar to that of the  $[\text{MeB}(\text{C}_6\text{F}_5)_3]^-$  analogue [33] except for the Cp resonances of **3**, which appear as two sharp equal-intensity resonances ( $\delta$  5.76 and 5.65) and not as only one broad Cp resonance ( $\delta$  5.70) [33], as it was observed in the latter case. These results confirm that the allyl ligand of **3** is indeed  $\eta^3$ -coordinated and relatively static at this temperature. When the sample temperature is increased, the coalescence of the Cp resonances occurs at about 60 °C. This translates into a free energy of activation for the intramolecular exchange processes of **3** of 68.6 kJ/mol, approximately 9 kJ/mol higher than the value estimated for the  $[\text{MeB}(\text{C}_6\text{F}_5)_3]^-$  analogue [33]. It seems likely that the increased free energy of activation in this case can be correlated with the increased electronegativity at the metal center, induced by the more weakly coordinating, less nucleophilic anion  $[\text{B}(\text{C}_6\text{F}_5)_4]^-$  vs.  $[\text{MeB}(\text{C}_6\text{F}_5)_3]^-$  [53–55], which would cause the  $\eta^3$ -allyl ligand of **3** to bind more tightly to the metal center, thus diminishing its fluxionality.

### 3.3. Formation of Zr-allyl species

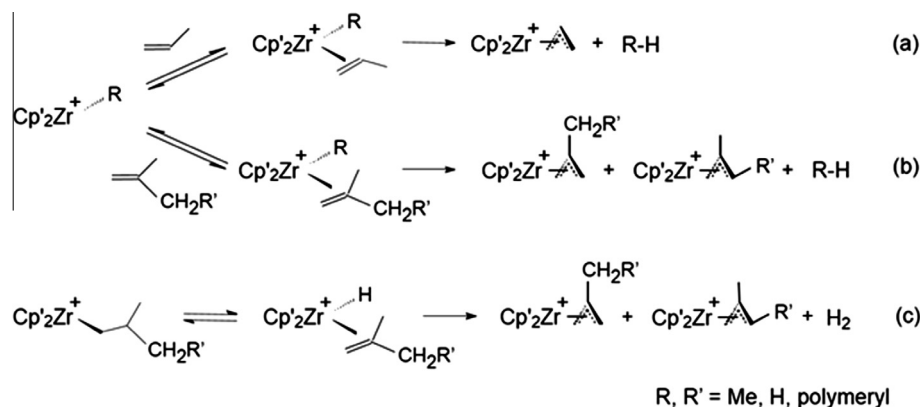
Three plausible pathways for the formation of  $\text{Cp}_2\text{Zr}^+$ -allyl species during propylene polymerization are depicted in Scheme 2. The first two, pathways (a) and (b), are somewhat similar and consist of coordination of alkene (propylene or the vinylidene end

group of a polypropylene chain released in solution following  $\beta$ -hydride elimination) to  $[\text{Cp}_2\text{ZrR}]^+$  ( $\text{R} = \text{Me}$ ,  $\text{H}$ , or polymeryl group), followed by intramolecular proton transfer from  $\text{C}_\gamma$  to the R ligand to yield a cationic zirconocene allyl complex  $\text{Cp}_2\text{Zr}^+$ -allyl and RH. Such reaction pathways find a precedent in alkene polymerization by organolanthanide complexes [22] as well as in reactions of 1,1-disubstituted alkenes  $\text{CH}_2=\text{C}(\text{Me})(\text{R})$  ( $\text{R} = \text{Me}$ , alkyl chain) with cationic zirconocene catalysts [24,25,33,35]. In pathway (c), which is supported by both computational [26,27] and experimental [34] studies, the coordinated alkene of a cationic zirconocene(hydride)(alkene) complex, obtained following  $\beta$ -hydride elimination of a cationic zirconocene-polypropenyl intermediate, does not dissociate but further transfers a  $\gamma$ -H to the hydride ligand to form a cationic zirconocene allyl species and release a dihydrogen molecule.

Here, the detection of methane in the  $^1\text{H}$  NMR spectra, along with the observation of oligomeric  $\text{Cp}_2\text{Zr}^+$ -allyl complexes in both the  $^1\text{H}$  NMR and electrospray ionization (tandem) mass spectra, suggests that the  $\text{Cp}_2\text{Zr}^+$ -allyl species were formed by (re)coordination of alkene to the cationic zirconocene catalyst and subsequent intramolecular  $\gamma$ -H transfer from the coordinated alkene to R (pathways (a) and (b) in Scheme 2). However, an additional reaction pathway in which  $\beta$ -H elimination of  $\text{Cp}_2\text{Zr}^+$ -polymeryl is followed directly by C–H activation, i.e., without prior alkene dissociation/recoordination (pathway (c) in Scheme 2), cannot be ruled out.

Indeed, recent studies [33] have demonstrated that vinylidene-terminated compounds, such as 2,4-dimethyl-1-pentene and 2,4-dimethyl-1-heptene, do react with **1** to form methane and cationic zirconocene allyl complexes. Remarkably, when **2** was employed as a catalyst in the reaction with 2,4-dimethyl-1-pentene [56], detailed low-temperature one- and two-dimensional  $^1\text{H}$  NMR spectroscopy experiments revealed that the reaction occurs via the transient  $[\text{Cp}_2\text{Zr}(\text{Me})(\text{CH}_2=\text{C}(\text{Me})\text{CH}_2\text{CHMe}_2)]^+$  species and that the coordinated alkene of this species assumes a near- $\eta^1$  structure (i.e., one in which  $\text{C}_\beta$  is almost carbocationic in nature) rather than the conventional  $\eta^2$  structure. In addition, the study also unveiled that the two terminal vinylidene hydrogens of the coordinated alkene undergo intramolecular exchange. The latter





**Scheme 2.** Possible reaction pathways for formation of  $\text{Cp}_2\text{Zr}^+$ -allyl species during zirconocene-catalyzed propylene polymerization.

was suggested to occur through the carbocationic complex  $\text{Cp}_2\text{Zr}(\text{Me})\text{CH}_2\text{C}^+(\text{Me})\text{CH}_2\text{CHMe}_2$ .

These observations are of fundamental interest, as they indicate that the vinylidene end groups of the polymer chains released in solution following  $\beta$ -hydride elimination reactions, although sterically unfavorable, can also re-coordinate to the vacant site at the metal center in a near  $\eta^1$  structure to form  $[\text{Cp}_2\text{Zr}(\text{R})(\text{CH}_2=\text{C}(\text{Me})\text{-polymeryl})]^+$ . The coordinated vinylidene group of the resulting metal-alkyl-alkene intermediate cannot insert, most likely because of steric hindrance. However, the strong polarization of the double bond in the near- $\eta^1$  coordinated vinylidene group allows rotation about the  $\text{C}_\alpha\text{-C}_\beta$  bond via the carbocationic complex  $\text{Cp}_2\text{Zr}(\text{R})\text{CH}_2\text{C}^+(\text{Me})\text{-polymeryl}$ ; the protons of the groups attached to  $\text{C}_\beta$  become strongly acidic, and therefore they can be more easily transferred to the R group on the metal center to form the corresponding Zr-allyl species and RH [56]. A corollary to this is that formation of metal-allyl intermediates in metallocene-catalyzed polymerizations of higher  $\alpha$ -olefins, i.e., those in which one hydrogen atom on  $\text{C}_\gamma$  is replaced by an alkyl group, would be more difficult for both steric and electronic reasons.

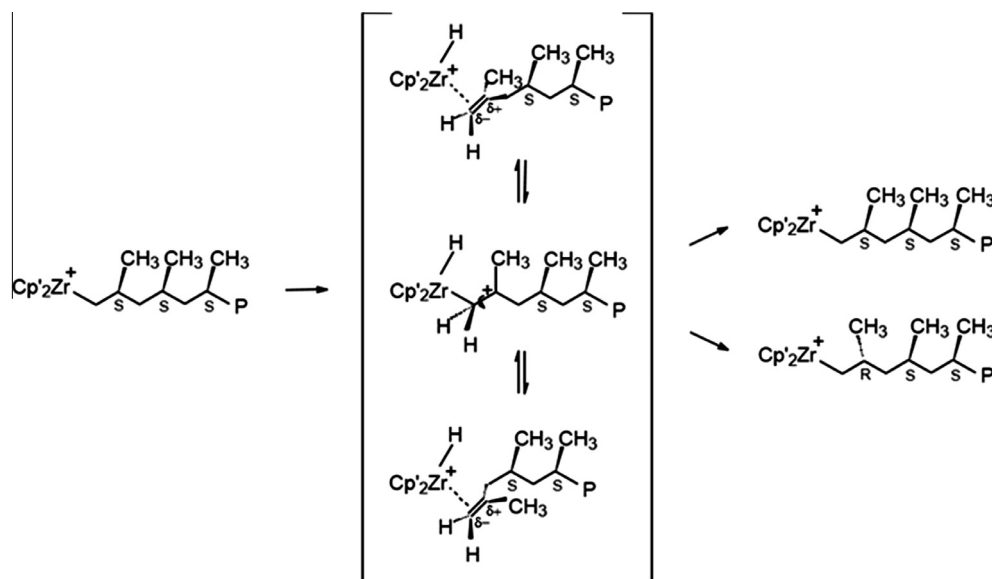
Noteworthy, aside from the intramolecular exchange of the two terminal vinylidene hydrogens of the coordinated alkene, the rotation about the  $\text{C}_\alpha\text{-C}_\beta$  bond of the vinylidene group of  $[\text{Cp}_2\text{Zr}(\text{Me})(\text{CH}_2=\text{C}(\text{Me})\text{CH}_2\text{CHMe}_2)]^+$  through the carbocationic species

$\text{Cp}_2\text{Zr}(\text{Me})\text{CH}_2\text{C}^+(\text{Me})(\text{CH}_2\text{CHMe}_2)$  also results in a reversal of the alkene enantioface relative to zirconium. In the context of propylene polymerization by metallocene catalysts, this can constitute a mechanism for chain end epimerization (see Scheme 3). Incorporation of stereoerrors within a polymer chain via the intermediacy of a carbocationic intermediate is expected to become predominant when the concentrations of propylene are reduced, consistent with earlier observations that polypropylene stereospecificity decreases when the polymerizations are run at low propylene concentrations [28,31]. This mechanism for stereoerror formation was not considered previously.

A kinetic study [57] on formation of cationic zirconium allyl species has shown that the reactions of 2,4-dimethyl-1-pentene with either **1** or **2** to form  $\text{Cp}_2\text{Zr}^+$ -allyl species in chlorobenzene- $\text{d}_5$ , follow a second order rate expression given by the equation

$$-d[\text{Cp}_2\text{Zr}^+\text{Me}]/dt = k[\text{Cp}_2\text{Zr}^+\text{Me}][2,4\text{-dimethyl-1-pentene}], \quad (3)$$

where  $k$  is the temperature-dependent rate constant for the reaction. The study indicated that the formation of  $\text{Cp}_2\text{Zr}^+$ -allyl species occurs with an activation energy between 46.4 and 50.9 kJ/mol [56,57]. Theoretical [58–60] and kinetic [61] studies on olefin polymerization by homogeneous metallocene catalysts, on the other hand, showed that the insertion of olefin into Zr-C  $\sigma$ -bonds during



**Scheme 3.** Probable mechanism for incorporation of stereoerrors into the polymer chain ( $\beta$ -hydride elimination, rotation about  $\text{C}_\alpha\text{-C}_\beta$  bond, reinsertion).



the propagation polymerization occurs with an activation energy between 25 and 30 kJ/mol. In this context, assuming that the pre-exponential factors are of about the same magnitude, the kinetic data suggest that the formation of Zr–allyl intermediates during the polymerization under the present reaction conditions may occur with a relative probability as often as one out of every 1000, as compared with olefin insertion, especially in systems where noncoordinating anions are used.

#### 3.4. Analysis of polymer chain unsaturation

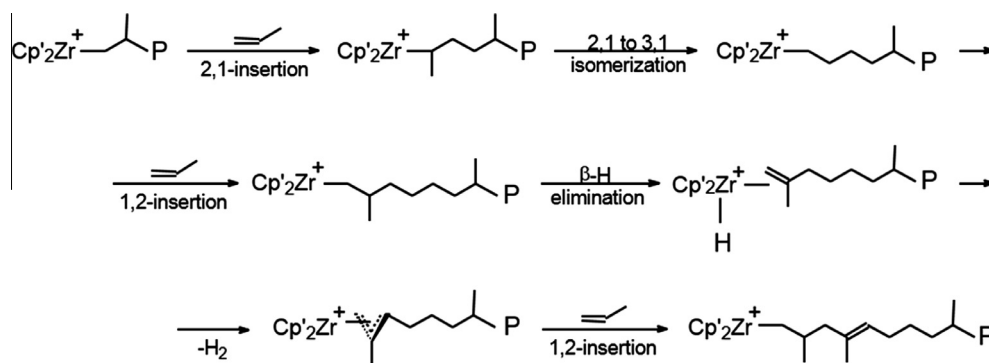
Studies on the reactivity of  $\text{Cp}'_2\text{Zr}^+$ –allyl ( $\text{Cp}' = \eta^5$ -cyclopentadienyl type group) complexes conducted by Lieber et al. [25] and Landis and Christianson [34] indicated that insertion of propylene and 1-hexene, respectively, proceeds much more slowly into a Zr–allyl bond than into a Zr–alkyl bond. Theoretical calculations by Ziegler and co-workers [26,27] showed that insertion of ethylene into a Zr–allyl bond can occur without substantial delay, and the authors have argued that for higher  $\alpha$ -olefins the insertion could be more difficult. Similar results were also obtained experimentally by Temme et al. [62], who found that a zirconocene–allyl borate–betaine system catalyzes the polymerization of ethylene more efficiently than that of propylene, whereas van der Heijden et al. [63] found that  $[(\text{C}_5\text{Me}_5)(\text{C}_5\text{H}_4\text{CMe}_3)\text{Zr}(\eta^3\text{-CH}_2\text{C}(\text{Me})\text{CH}_2)]^+$  is reactive toward ethylene but does not react with  $\alpha$ -olefins.

Subsequent propylene insertion into the Zr–allyl bond of an oligomeric  $\text{Cp}'_2\text{Zr}^+$ –allyl intermediate would invariably lead to incorporation of internal unsaturation within the polymer chain [64,65]. Therefore, an analysis of polymer chain unsaturation would indicate whether the  $\text{Cp}'_2\text{Zr}^+$ –allyl intermediates formed during catalysis are reactive toward propylene.

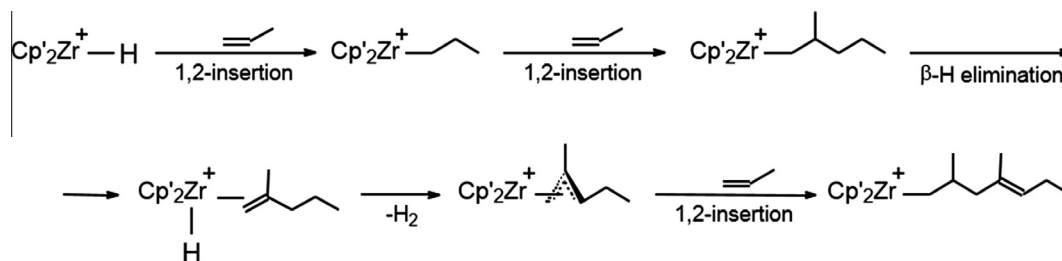
The olefinic region of the  $^1\text{H}$  NMR spectra of the reaction mixtures obtained from propylene polymerization by **1** (Fig. 1) shows the presence of multiple resonances between  $\delta$  4.78 and 4.94 as well as of a triplet resonance at  $\delta \sim 5.2$  ( $J_{\text{HH}} = 7$  Hz). On the basis of comparison with literature data [43,44], the resonances

between  $\delta$  4.78 and 4.94 were attributed to the vinylidene end groups and possibly internal vinylidene groups of different lengths, short-chain atactic polypropylene oligomers. A terminal vinylidene group arises from  $\beta$ -hydride elimination following a primary (1,2) propylene insertion into Zr–alkyl chains, while an internal vinylidene group is the result of propylene insertion into a Zr–allyl bond [44,53,54]. The resonance at  $\delta \sim 5.2$  was attributed to the vinylic proton of an internal unsaturation group of the type  $-\text{CH}_2\text{CH}_2\text{CH}=\text{C}(\text{CH}_3)-$  [44,66]. As noted by Resconi et al. [44,46], a similar triplet resonance at  $\delta \sim 5.2$  has been observed previously in the  $^1\text{H}$  NMR spectra of isotactic polypropylene. For the reason that this resonance was noticed to arise only in conjunction with the *cis*-2-butenyl end group resonance at  $\delta \sim 5.4$  [65], it was proposed to be connected to the presence of secondary (2,1) insertions [44,66]; yet no mechanism has been suggested. A plausible mechanism that would account for the occurrence of an internal olefinic group of the type  $-\text{CH}_2\text{CH}_2\text{CH}=\text{C}(\text{CH}_3)-$  on the polymer chain is presented in Scheme 4 and would involve the presence of a Zr–allyl species in addition to a secondary (2,1) Zr–alkyl intermediate.

However, while isotactic polypropylene is known to incorporate small amounts of regiodefects as a result of occasional secondary propylene insertions [44], so far there are no reports indicating the presence of secondary insertions in atactic polypropylene [15]. An alternative mechanism that might explain the incorporation of an internal olefinic group of the type  $-\text{CH}_2\text{CH}_2\text{CH}=\text{C}(\text{Me})(\text{R})$  ( $\text{R} = \text{alkyl group}$ ) into the polymer chain is shown in Scheme 5. Here, the cationic  $\text{Cp}'_2\text{Zr}^+-\text{CH}_2\text{CH}(\text{Me})\text{CH}_2\text{CH}_2\text{CH}_3$  species, obtained following two consecutive primary (1,2) insertions of propylene into the  $\text{Cp}'_2\text{Zr}^+-\text{H}$  bond, undergoes  $\beta$ -hydride elimination followed by allylic C–H activation of the coordinated vinylidene chain end at the methylene group to form a cationic  $\text{Cp}'_2\text{Zr}^+(\eta^3\text{-CH}_2\text{C}(\text{Me})\text{CHCH}_2\text{CH}_3)$  species. Subsequent propylene insertion into the new Zr–allyl bond would result in a polymer chain with a  $\text{CH}_3\text{CH}_2\text{CH}=\text{C}(\text{Me})-$  end group. The presence of a 3-propenyl end group on polypropylene chains has not been considered previously.



**Scheme 4.** Possible mechanism for formation of an internal olefinic group of the type  $-\text{C}(\text{Me})=\text{CHCH}_2\text{CH}_2\text{CH}_2-$ .



**Scheme 5.** Possible mechanism for formation of a  $\text{CH}_3\text{CH}_2\text{CH}=\text{C}(\text{Me})-$  end group.



Thus, this latter mechanism shows that the presence of a triplet resonance at  $\delta \sim 5.2$  in the  $^1\text{H}$  NMR spectra of polypropylene can be connected with the presence of Zr–allyl intermediates only and does not necessarily need the presence of a secondary insertion. Indeed, the  $^1\text{H}$  NMR spectra of in situ propylene polymerization by **1** (Fig. 1) also show the presence of allylic resonances between  $\delta$  2.5 and 4.8, in addition to the olefinic resonances between  $\delta$  4.78 and 4.94. Also, a closer examination of the  $^1\text{H}$  NMR spectra of isotactic polypropylene in references [44,46] indicates the presence of internal vinylidene groups, which were ascribed to the presence of Zr–allyl species during the polymerization, in addition to the triplet resonance at  $\delta$  5.2; yet no connection between the presence of the triplet at  $\delta$  5.2 and that of internal vinylidene groups was made.

No olefinic hydrogen resonances were detected in the  $^1\text{H}$  NMR spectra of the in situ reaction of propylene with **2** (see Fig. 4). This observation, coupled with the observation that allylic hydrogen resonances are present between  $\delta$  2.5 and 4.7, implies that the insertion of propylene into the Zr–allyl bond in this case is more difficult, consistent with the finding that zirconium–allyl interaction is stronger in this case (vide supra).

#### 4. Summary

Cationic  $\text{Cp}_2\text{Zr}^+$ –allyl species were detected in the reaction mixture of  $\text{Cp}_2\text{ZrMe}_2$  activated by either  $\text{B}(\text{C}_6\text{F}_5)_3$  or  $[\text{Ph}_3\text{C}][\text{B}(\text{C}_6\text{F}_5)_4]$  and propylene by  $^1\text{H}$  NMR spectroscopy. Furthermore, short-chain oligomeric  $\text{Cp}_2\text{Zr}^+$ –polymeryl and  $\text{Cp}_2\text{Zr}^+$ –allyl species were also detected, for the first time, directly from the reaction mixture of  $\text{Cp}_2\text{ZrMe}_2$  activated by  $\text{B}(\text{C}_6\text{F}_5)_3$  and propylene by electrospray ionization (tandem) mass spectrometry. The formation of  $\text{Cp}_2\text{Zr}^+$ –allyl species occurs via coordination of alkene (propylene and vinylidene end groups of unsaturated polymer chains, respectively) to the active catalyst  $\text{Cp}_2\text{Zr}^+\text{R}$  ( $\text{R} = \text{CH}_3$ , H, polymeryl chain), followed by intramolecular proton transfer from  $\text{C}\gamma$  to R and release of RH; however, an additional mechanism in which  $\beta$ -H elimination of  $\text{Cp}_2\text{Zr}^+$ –polymeryl is followed directly by  $\gamma$ -H elimination to form  $\text{Cp}_2\text{Zr}^+$ –allyl along with  $\text{H}_2$  cannot be discounted.

Analysis of the olefinic region of the  $^1\text{H}$  NMR spectra of the reaction mixture obtained from **1** and propylene reveals the presence of a triplet resonance at  $\delta \sim 5.2$ . This was attributed to the olefinic proton of the unprecedented 3-propenyl end group. A plausible mechanism for the origin of the 3-propenyl end groups of the unsaturated polymer chains is discussed. Additionally, a mechanism for the incorporation of stereodeflects in stereoregular polymers, via the intermediacy of the carbocationic species  $\text{Cp}_2\text{Zr}(\text{H})(\text{CH}_2\text{C}^+(\text{Me})\text{--polymeryl})$ , is advanced. The cationic  $\text{Cp}_2\text{Zr}^+$ –allyl intermediates formed during polymerization may contribute to catalyst deactivation.

#### Acknowledgments

Financial support from Queen's University is gratefully acknowledged. I thank Dr. Françoise Sauriol for her assistance with NMR spectroscopy and Dr. Bernd O. Keller for his help with mass spectrometry. I also thank Prof. Richard F. Jordan (University of Chicago), Prof. Clark R. Landis (University of Wisconsin–Madison), and Prof. Natalie M. Cann for helpful discussions.

#### References

- [1] W. Kaminsky, *Macromol. Chem. Phys.* 197 (1996) 3907.
- [2] G.W. Coates, *Chem. Rev.* 100 (2000) 1223.
- [3] H.-H. Brintzinger, D. Fischer, R. Mülhaupt, B. Rieger, R.M. Waymouth, *Angew. Chem., Int. Ed. Engl.* 34 (1995) 1143.
- [4] P.C. Möhring, N.J. Coville, *J. Organomet. Chem.* 479 (1994) 1.
- [5] W. Kaminsky, *J. Chem. Soc., Dalton Trans.* (1998) 1413.
- [6] L. Resconi, L. Cavallo, A. Fait, F. Piemontesi, *Chem. Rev.* 100 (2000) 1253.
- [7] M. Bochmann, *J. Chem. Soc., Dalton Trans.* (1996) 255.
- [8] E.Y.-X. Chen, T.J. Marks, *Chem. Rev.* 100 (2000) 1391.
- [9] X. Yang, C.L. Stern, T.J. Marks, *J. Am. Chem. Soc.* 113 (1991) 3623.
- [10] X. Yang, C.L. Stern, T.J. Marks, *J. Am. Chem. Soc.* 116 (1994) 10015.
- [11] J.C.W. Chien, W.-M. Tsai, M.D. Rausch, *J. Am. Chem. Soc.* 113 (1991) 8570.
- [12] X. Yang, C.L. Stern, T.J. Marks, *Organometallics* 10 (1991) 840.
- [13] J.C.W. Chien, R. Sugimoto, *J. Polym. Sci., Part A: Polym. Chem.* 29 (1991) 459.
- [14] M. Bochmann, *Top. Catal.* 7 (1999) 9.
- [15] M. Vatananu, B.N. Boden, M.C. Baird, *Macromolecules* 38 (2005) 9944.
- [16] K.A. Novstrup, N.E. Travia, G.A. Medvedev, C. Stanciu, J.M. Switzer, K.T. Thomson, W.N. Delgass, M.M. Abu-Omar, J.M. Caruthers, *J. Am. Chem. Soc.* 132 (2010) 558.
- [17] B.M. Moscatto, B. Zhu, C.R. Landis, *Organometallics* 31 (2012) 2097.
- [18] V. Busico, R. Cipullo, J.C. Chadwick, J.F. Modder, O. Sudmeijer, *Macromolecules* 27 (1994) 7538.
- [19] V. Busico, R. Cipullo, G. Talarico, L. Caporaso, *Macromolecules* 31 (1998) 2387.
- [20] S. Lin, R. Kravchenko, R.M. Waymouth, *J. Mol. Catal. A: Chem.* 158 (2000) 423.
- [21] V. Busico, R. Cipullo, S. Ronca, *Macromolecules* 35 (2002) 1537.
- [22] G. Jeske, H. Lauke, H. Mauermann, P.N. Swepston, H. Schumann, T.J. Marks, *J. Am. Chem. Soc.* 107 (1985) 8091.
- [23] J.J.W. Eshuis, Y.Y. Tan, A. Meetsma, J.H. Teuben, J. Renkema, G.G. Evens, *Organometallics* 11 (1992) 362.
- [24] A.D. Horton, *Organometallics* 15 (1996) 2675.
- [25] S. Lieber, M.-H. Prosenc, H.-H. Brintzinger, *Organometallics* 19 (2000) 377.
- [26] P.M. Margl, T.K. Woo, T. Ziegler, *Organometallics* 17 (1998) 4997.
- [27] C. Zhu, T. Ziegler, *Inorg. Chim. Acta* 345 (2003) 1.
- [28] M.K. Leclerc, H.-H. Brintzinger, *J. Am. Chem. Soc.* 118 (1996) 9024.
- [29] M.-H. Prosenc, H.-H. Brintzinger, *Organometallics* 16 (1997) 3889.
- [30] L. Resconi, *J. Mol. Catal. A: Chem.* 146 (1999) 167.
- [31] J.C. Yoder, J.E. Bercaw, *J. Am. Chem. Soc.* 124 (2002) 2548.
- [32] D.R. Sillars, C.R. Landis, *J. Am. Chem. Soc.* 125 (2003) 9894.
- [33] M. Vatananu, *Organometallics* 33 (2014) 3683.
- [34] C.R. Landis, M.D. Christianson, *Proc. Natl. Acad. Sci. USA* 103 (2006) 15349.
- [35] A. Al-Humyidi, J.C. Garrison, M. Mohammed, W.J. Youngs, S. Collins, *Polyhedron* 24 (2005) 1234.
- [36] D.E. Babushkin, V.N. Panchenko, H.-H. Brintzinger, *Angew. Chem., Int. Ed.* 53 (2014) 9645.
- [37] E.P. Talsi, J.L. Eilertsen, M. Ystenes, E. Rytter, *J. Organomet. Chem.* 677 (2003) 10.
- [38] E. Samuel, M.D. Rausch, *J. Am. Chem. Soc.* 95 (1973) 6263.
- [39] W.E. Hunter, D.C. Hrnčir, R.V. Bynum, R.A. Penttilä, J.L. Atwood, *Organometallics* 2 (1983) 750.
- [40] A.G. Massey, A.J. Park, *J. Organomet. Chem.* 2 (1964) 245.
- [41] H. Günther, *NMR Spectroscopy: Basic Principles, Concepts, and Applications in Chemistry*, second ed., Wiley, Chichester, UK, 1995.
- [42] G.R. Fulmer, A.J.M. Miller, N.H. Sherdn, H.E. Gottlieb, A. Nudelman, B.M. Stoltz, J.E. Bercaw, K.I. Goldberg, *Organometallics* 29 (2010) 2176.
- [43] R.M. Silverstein, F.X. Webster, *Spectrometric Identification of Organic Compounds*, sixth ed., Wiley, 1998.
- [44] L. Resconi, I. Camurati, O. Sudmeijer, *Top. Catal.* 7 (1999) 145.
- [45] S.R. Wilson, Y. Wu, *Organometallics* 12 (1993) 1478.
- [46] L.S. Santos, J.O. Metzger, *Angew. Chem., Int. Ed.* 45 (2006) 977.
- [47] C.S. Christ Jr., J.R. Eyler, D.E. Richardson, *J. Am. Chem. Soc.* 112 (1990) 596.
- [48] A.A. Aksenov, C.S. Contreras, D.E. Richardson, J.R. Eyler, *Organometallics* 26 (2007) 478.
- [49] D. Feichtinger, D.A. Plattner, P. Chen, *J. Am. Chem. Soc.* 120 (1998) 7125.
- [50] M. Bochmann, S.J. Lancaster, *Angew. Chem., Int. Ed. Engl.* 33 (1994) 1634.
- [51] M.-C. Chen, J.A.S. Roberts, T.J. Marks, *J. Am. Chem. Soc.* 126 (2004) 4605.
- [52] J. Zhou, S.J. Lancaster, D.A. Walker, S. Beck, M. Thornton-Pett, M. Bochmann, *J. Am. Chem. Soc.* 123 (2001) 223.
- [53] L. Jia, X. Yang, C.L. Stern, T.J. Marks, *Organometallics* 16 (1997) 842.
- [54] Y.-X. Chen, M.V. Metz, L. Li, C.L. Stern, T.J. Marks, *J. Am. Chem. Soc.* 120 (1998) 6287.
- [55] F. Song, S.J. Lancaster, R.D. Cannon, M. Schormann, S.M. Humphrey, C. Zuccaccia, A. Macchioni, M. Bochmann, *Organometallics* 24 (2005) 1315.
- [56] M. Vatananu, G. Stojcevic, M.C. Baird, *J. Am. Chem. Soc.* 130 (2008) 454.
- [57] M. Vatananu, The activation parameters for Zr–allyl formation from **1** and 2,4-dimethyl-1-pentene are  $\Delta H^\ddagger = 48.3$  kJ/mol and  $\Delta S^\ddagger = -72.5$  J/mol K, while those for Zr–allyl formation from **2** and 2,4-dimethyl-1-pentene are  $\Delta H^\ddagger = 44.4$  kJ/mol and  $\Delta S^\ddagger = -42.4$  J/mol K (unpublished data).
- [58] T. Yoshida, N. Koga, K. Morokuma, *Organometallics* 14 (1995) 746.
- [59] T. Yoshida, N. Koga, K. Morokuma, *Organometallics* 15 (1996) 766.
- [60] P. Margl, L. Deng, T. Ziegler, *J. Am. Chem. Soc.* 120 (1998) 5517.
- [61] J.C.W. Chien, A. Razavi, *J. Polym. Sci., Part A: Polym. Chem.* 26 (1988) 2369.
- [62] B. Temme, G. Erker, J. Karl, H. Luftmann, R. Fröhlich, S. Kotila, *Angew. Chem., Int. Ed. Engl.* 34 (1995) 1755.
- [63] H. van der Heijden, B. Hessen, A.G. Orpen, *J. Am. Chem. Soc.* 120 (1998) 1112.
- [64] G. Moscardi, L. Resconi, L. Cavallo, *Organometallics* 20 (2001) 1918.
- [65] C.J. Schaverien, R. Ernst, P. Schut, T. Dall'Occo, *Organometallics* 20 (2001) 3436.
- [66] L. Resconi, F. Piemontesi, I. Camurati, O. Sudmeijer, I.E. Nifant'ev, P.V. Ivchenko, L.G. Kuz'mina, *J. Am. Chem. Soc.* 120 (1998) 2308.